Received: 17 October 2018 | Revised: 21 March 2019 | Accepted: 25 March 2019

DOI: 10.1111/gcb.14632

PRIMARY RESEARCH ARTICLE

Global Change Biology WILEY

Dissecting the nonlinear response of maize yield to high temperature stress with model-data integration

Peng Zhu[1,2] | Qianlai Zhuang[1,3] | Sotirios V. Archontoulis[4] | Carl Bernacchi[5,6] | Christoph Müller[7]

[1]Department of Earth, Atmospheric, and Planetary Sciences, Purdue University, West Lafayette, Indiana

[2]School of Global Policy and Strategy, University of California San Diego, La Jolla, California

[3]Department of Agronomy, Purdue University, West Lafayette, Indiana

[4]Department of Agronomy, Iowa State University, Ames, Iowa

[5]Department of Plant Biology, University of Illinois at Urbana-Champaign, Urbana, Illinois

[6]Global Change and Photosynthesis Research Unit, USDA-ARS, Urbana, Illinois

[7]Potsdam Institute for Climate Impact Research (PIK), Potsdam, Germany

Correspondence
Qianlai Zhuang, Department of Earth, Atmospheric, and Planetary Sciences, Purdue University, West Lafayette, IN.
Email: qzhuang@purdue.edu

Funding information
National Science Foundation, Grant/Award Number: IIS - 1027955; NASA, Grant/Award Number: NNX09AI26G

Abstract

Evidence suggests that global maize yield declines with a warming climate, particularly with extreme heat events. However, the degree to which important maize processes such as biomass growth rate, growing season length (GSL) and grain formation are impacted by an increase in temperature is uncertain. Such knowledge is necessary to understand yield responses and develop crop adaptation strategies under warmer climate. Here crop models, satellite observations, survey, and field data were integrated to investigate how high temperature stress influences maize yield in the U.S. Midwest. We showed that both observational evidence and crop model ensemble mean (MEM) suggests the nonlinear sensitivity in yield was driven by the intensified sensitivity of harvest index (HI), but MEM underestimated the warming effects through HI and overstated the effects through GSL. Further analysis showed that the intensified sensitivity in HI mainly results from a greater sensitivity of yield to high temperature stress during the grain filling period, which explained more than half of the yield reduction. When warming effects were decomposed into direct heat stress and indirect water stress (WS), observational data suggest that yield is more reduced by direct heat stress (−4.6 ± 1.0%/°C) than by WS (−1.7 ± 0.65%/°C), whereas MEM gives opposite results. This discrepancy implies that yield reduction by heat stress is underestimated, whereas the yield benefit of increasing atmospheric CO_2 might be overestimated in crop models, because elevated CO_2 brings yield benefit through water conservation effect but produces limited benefit over heat stress. Our analysis through integrating data and crop models suggests that future adaptation strategies should be targeted at the heat stress during grain formation and changes in agricultural management need to be better accounted for to adequately estimate the effects of heat stress.

KEYWORDS
crop model, crop phenological stages, harvest index, high temperature stress, satellite observations, water stress

Abbreviations: AGB, aboveground biomass; An, anthesis; BGR, daily biomass growth rate, AGB divided by growing season length; ET, evapotranspiration; GDD, growing degree days; GFP, grain filling period; GSL, growing season length; HDD, high temperature degree days; HDD^{VP}, HDD^{An} and HDD^{GFP}, HDD during vegetative period, anthesis and GFP; HI, harvest index, yield/AGB; IWDRVI, integrated wide dynamic range vegetation index; MEM, model ensemble mean; PET, potential evapotranspiration; S_T^{Yield}, S_T^{BGR}, S_T^{GSL} and S_T^{HI}, temperature sensitivity of yield, BGR, GSL and HI; VP, vegetative period; WDRVI, wide dynamic range vegetation index; WS, water stress.

1 | INTRODUCTION

As the world's largest producer of maize, the United States has seen a steady increase in maize yield since the Green Revolution (Assefa et al., 2017), while increases in concurrent heat and drought across the United States since the 1950s have posed a significant risk for maize production (Mazdiyasni and AghaKouchak, 2015; Schauberger et al., 2017) and resulted in stagnated crop production in many producing areas (Olesen et al., 2011). Future warming might more severely decrease crop yield with frequent extreme heat events (Rahmstorf, & Coumou, 2011; Schlenker & Roberts, 2009), which causes oxidative damage to chloroplasts (Crafts-Brandner & Salvucci 2002; Siebers, Yendrek, & Drag, 2015), destroys reproductive structures (Commuri & Jones, 2001), and accelerates crop senescence (Lobell, Sibley, & Ivan Ortiz-Monasterio, 2012; Ruiz-Vera, Siebers, Jaiswal, Ort, & Bernacchi, 2018). With warmer climates, current agricultural system models need to be upgraded to better represent crop responses to temperature-related climate extremes and thus cope with the upcoming challenges of increasing food demands.

In recent decades, multiple approaches have been adopted to maintain yield increases through improved management practices and breeding technology, like improved herbicide and weed management techniques, higher planting density, and new cultivars with longer grain filling period (GFP) (Assefa et al., 2016; Tao, Yokozawa, Xu, Hayashi, & Zhang, 2006; Tollenaar & Wu, 1999; Zhu et al., 2018). However, the actual effects of these intensified management practices might be counterproductive due to the diverse environmental conditions and their interaction with management practices (Lobell et al., 2014). Therefore, it is necessary to better understand the response of crop yield to climatic variation in field conditions.

The observed variation in maize yield is the product of many interactive processes that make a mechanistic understanding of the drivers of this variation difficult. Throughout the life cycle of maize plants, yield is driven by biomass accumulation and partitioning between organs (Lizaso et al., 2018). Biomass accumulation can be expressed as growing season length (GSL) × average daily biomass growth rate (BGR). The partitioning of biomass to grains is often quantified using harvest index (HI = yield/above-ground biomass accumulation). Thus, final yield is the product of BGR, GSL and HI. Warming influence on maize yield can be thereby dissected as the influence on GSL, BGR and HI. Warmer temperature often means a shorter GSL with accelerated development rate (Cheikh & Jones, 1994). However, the influence of warming on BGR and HI is more complex than GSL. The direction and magnitude of influence depend on whether the threshold temperature has been exceeded, while the threshold temperature seems to be variable among different varieties and phenological stages (Rezaei, Webber, Gaiser, Naab, & Ewert, 2015; Sánchez, Rasmussen, & Porter, 2014).

As a C_4 plant, maize often has a higher optimal temperature for photosynthesis than C_3 plants, thus warmer leaf temperatures in early vegetative growth can potentially lead to either no impacts or a positive impact on maize photosynthetic activity (Crafts-Brandner & Salvucci, 2002; Parent & Tardieu, 2012). However, maize yield becomes increasingly sensitive to high temperature during reproductive development (Cheikh & Jones, 1994; Siebers et al., 2017). Thus, the same level of warming treatment in different stages might result in different or even opposite influence on maize yield (Siebers et al., 2017). In particular, identifying cropping system vulnerabilities and devising targeted adaptation strategies to deal with future warming should be on the premise of a clear understanding of how crop yields respond to warming during different development stages. Due to limited knowledge of crop stages (Butler & Huybers, 2015), analyses on the sensitivity of crop yields to temperature typically ignore that the response to temperature is stage dependent (Cheikh & Jones, 1994; Siebers et al., 2017). This might lead to considerable uncertainty when projecting crop yield under future warmer climate.

Field warming experiments have been devised to explore the effects of warming in different growth stages on crop yield (Hatfield & Prueger, 2015; Ruiz-Vera et al., 2018; Siebers et al., 2017). It has been suggested that maize grain yield is significantly reduced under heat stress through pollen viability that in turn determines kernel number and HI, which explained most of the variation in maize yield (Edreira & Otegui, 2012, 2013; Lizaso et al., 2018). In terms of the timing of heating treatment, it appears that kernel number per plant was more reduced by heating during silking than before anthesis (Edreira & Otegui, 2012). Influence of heating on phenological development is also evident. Grain yield was significantly reduced due to shortening of GFP when temperatures were increased from 25°C to 31°C, despite the enhanced grain filling rate (Dias & Lidon, 2009). Heating during pre-silking caused a larger delay in silking date than in anthesis date, leading to a lengthened anthesis-silking interval (Cicchino, Rattalino Edreira, Uribelarrea, & Otegui, 2010), which is a good indicator of the final maize yield (Bolanos & Edmeades, 1996). However, these experiments are often limited to small scales and could not represent the complex and diverse crop systems, making the conclusion hard to be extrapolated to other regions.

Crop models have shown the potential to simulate and reproduce the large-scale spatiotemporal variability of crop yield (Elliott et al., 2015; Müller et al., 2017). Generally, crop models represent our understanding of response of crop plants to climatic variation, soil nutrient status, hydrological conditions, and agronomic management practices. They are normally able to adequately simulate average conditions but fail to handle climate extremes (Eitzinger et al., 2013; Lobell et al., 2012; Sánchez et al., 2014). Such limitation is critical to evaluate crop response under ongoing climatic change, which is expected to bring more extreme weather for the agricultural sector across the world. In addition, some basic knowledge might have not been updated for decades. For example, the default parameters related to the physiological property of crop varieties might be unable to reflect the recent progress in cultivars through breeding techniques. Thus, it might bring substantial uncertainties

when using these models to reproduce historic or project future crop yield. Recently, an ensemble of multi-model output has been widely used as an improved way of evaluating and projecting climate change and management effects on crop production with reduced uncertainty (Asseng et al., 2014; Rötter, Carter, Olesen, & Porter, 2011).

New techniques employing satellite data have been increasingly used in the agricultural sector to map crop types, delineate irrigation/non-irrigation boundary, derive crop phenology information, and project field crop yield (Azzari, Jain, & Lobell, 2017; Deines, Kendall, & Hyndman, 2017; Guan et al., 2017; Lobell, Thau, Seifert, Engle, & Little, 2015; Zhu et al., 2018). Such observational information could be important input data to drive crop models or calibrate model parameters. The derived crop phenology information is likely to provide observational evidence to characterize the regional-scale spatiotemporal patterns of field crop growth status (Zhu et al., 2018) and thus assist the understanding of response of crop yield to climatic variation during different growth stages.

Here we integrated satellite-derived crop stage information, regional crop model output, surveyed yield data from the United States Department of Agriculture (USDA) and site-level experiment data to dissect how high temperatures influence maize yield through different physiological processes. Surveyed yield data, together with satellite-based crop stage information and modeled maize aboveground biomass (AGB) calibrated against site-measured AGB, enabled us to retrieve county-level GSL, BGR (AGB/GSL) and HI (Yield/AGB). This was used to decompose the temperature sensitivity of yield (S_T^{Yield}) into the temperature sensitivities of BGR (S_T^{BGR}), GSL (S_T^{GSL}), and HI (S_T^{HI}), which were estimated with a panel model (Schauberger et al., 2017; Schlenker & Roberts, 2009; Tack, Barkley, & Nalley, 2015). Each component characterizes the temperature response of net assimilation rate determined by photosynthesis and respiration (S_T^{BGR}), plant development rate (S_T^{GSL}), and reproductive growth determined by grain size and grain weight (S_T^{HI}), respectively. In addition, S_T^{Yield}, S_T^{BGR}, S_T^{GSL}, and S_T^{HI} based on multiple crop model outputs were also analyzed to complement the survey and satellite data. The relative contribution of direct heat stress and indirect water stress (WS) to yield reduction was further estimated using statistical model and crop model simulation to investigate the underlying driver of maize yield reduction with climatic warming. In this study, we focused on three Midwest states dominated by rainfed maize—Indiana, Illinois, and Iowa—that account for approximately 40% of U.S. maize production (USDA, 2015). Thus, the conclusions drawn from this study are likely to provide insight for understanding the temperature response of the whole U.S. rainfed maize production.

2 | MATERIALS AND METHODS

2.1 | Satellite data derived crop stage information

In this study, 8-day time series of 250 m daily surface reflectance MODIS datasets on board Earth Observing System (EOS) Terra and Aqua satellite platforms: MOD09Q1 (2000–2015) and MYD09Q1 (2002–2015) Collection 6, were used. Here a scaled wide dynamic range vegetation index (WDRVI) was used to monitor the growing status of maize plants (Gitelson, 2004), because WDRVI has a higher sensitivity to changes at moderate to high biomass than the normalized difference vegetation index (NDVI). The scaled WDRVI is calculated with the following equation:

$$NDVI = (\rho_{NIR} - \rho_{red}) / (\rho_{NIR} + \rho_{red}) \quad (1)$$

$$\mathrm{WDRVI} = 100 \times \frac{[(\alpha - 1) + (\alpha + 1) \times \mathrm{NDVI}]}{[(\alpha + 1) + (\alpha - 1) \times \mathrm{NDVI}]} \quad (2)$$

where ρ_{red} and ρ_{NIR} are the MODIS surface reflectance in the red and NIR bands, respectively. The scaling factor α is introduced to degrade the fraction of the NIR reflectance at moderate-to-high green vegetation (Guindin-Garcia, Gitelson, Arkebauer, Shanahan, & Weiss, 2012). Here α was set as 0.1 as a comparison of multiple vegetation indexes indicates WDRVI with α = 0.1 showed a strong linear correlation with corn green LAI (Guindin-Garcia et al., 2012). Before WDRVI calculation, the reflectance data were quality-filtered using the quality control flags. Only the data passing the highest quality control test are retained. A hybrid method combining shape model fitting (SMF) and threshold-based analysis was implemented to derive maize phenology using MODIS WDRVI data at 250 × 250 m spatial resolution from 2000 to 2015 (Zhu et al., 2018). Shape model was obtained by averaging multiple years WDRVI observations to characterize the climatology of corn growth cycle (Zhu et al., 2018). The shape model was then geometrically scaled to fit each WDRVI time series, so the predefined phenological dates on the shape model can be scaled likewise to estimate phenological dates for each pixel. We have derived four key maize growth stages of emergence (late May), silking (Middle July), dent (late August), and maturity (late September) across the four states: Indiana, Illinois, Iowa, and Nebraska. Verification at the state level showed a good agreement between MODIS-derived maize phenology and the National Agricultural Statistics Service (NASS)–reported state mean phenological dates (Zhu et al., 2018). In this study, we focused on the three rainfed states: Iowa, Illinois, and Indiana.

2.2 | Derivation of county-level maize yield, AGB, GSL, and HI

The observed variation in maize yield is the end result of integration of many processes with different sensitivities to high temperature stress. To this end, we decompose the total yield variation into three components: BGR, GSL, and HI. County-level corn grain yield dataset from 2000 to 2015 covering the three states (Illinois, Indiana, Iowa) was retrieved from the Quick Stats 2.0 database. The unit system for maize yield is bushel per acre (bu/ac). This dataset was used together with remote sensing modeled county-level AGB to estimate HI (Yield/AGB). HI generally characterizes dry matter partitioning between source organ and sink organ and

is mainly related to processes determining grain size and grain weight.

Thirty-two site-year maize AGB data measured at the end of growing season across the U.S. Midwest were collected (details on geolocation and year information can be found in Table S1). This field experiment measurement was used to construct a regression model between WDRVI and AGB. To this end, WDRVI in 3 × 3 pixel windows centered on the site measured AGB was obtained and a quality control procedure was applied to the WDRVI time series to remove low-quality, cloud/aerosol-contaminated observations. Pearson correlation was then estimated between the WDRVI time series centered on the site and the surrounding eight pixels. Three WDRVI time series scoring the highest correlation and the center one were averaged for constructing the regression model. Previous studies have showed the integrated enhanced vegetation index (EVI) over the growing season is a good proxy of vegetation AGB (Ponce-Campos et al., 2013). Similarly, we integrated WDRVI (IWDRVI) by summing WDRVI over the growing season, which was based on the previous study-retrieved phenology dates (Zhu et al., 2018). A linear regression model was constructed between in situ measured AGB and processed IWDRVI with the above method. The model shows IWDRVI has a good explaining power (R^2 = 0.75, p < 0.0001) with the equation: AGB = $(16.4 \pm 2.5) * \text{IWDRVI}^{(0.8 \pm 0.08)}$ (±SE) (Figure 1). We also applied the same procedure to NDVI and enhanced vegetation index 2 (EVI2), which are also commonly used vegetation indexes for temporal monitoring of vegetation greenness and productivity, but the R^2 of NDVI (R^2 = 0.68) and EVI2 (R^2 = 0.64) is lower than the one using WDRVI as the predictor. With this regression model, AGB was spatially estimated with satellite-retrieved IWDRVI. Finally, the 16 years of satellite data derived GSL and AGB were integrated to county level to estimate HI (Yield/AGB) and daily BGR (AGB/GSL) for each county.

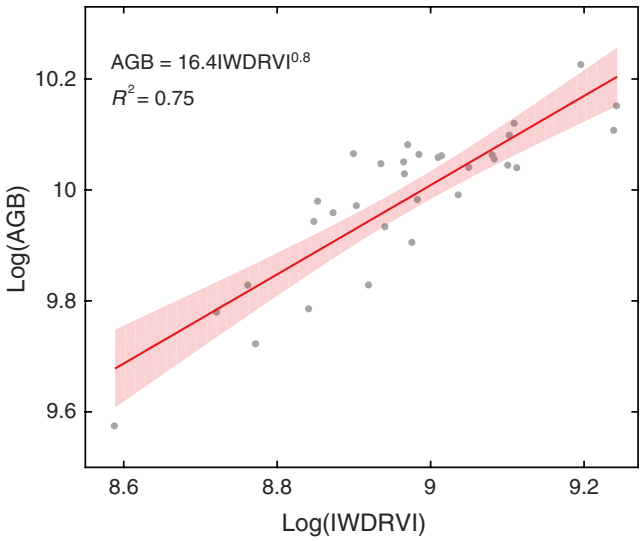

FIGURE 1 The regression model used to relate the integrated wide dynamic range vegetation index (IWDRVI) with aboveground biomass (AGB). Each point corresponds to a site-measured AGB and MODIS-derived IWDRVI. The shaded area indicates the 95% confidence interval

2.3 | Statistical analysis of temperature sensitivity across different growth stages

Temperature sensitivity of maize yield (S_T^{Yield}) was estimated using a panel data model (Equation 3) with growing season mean surface air temperature (Tsa) and precipitation (Prcp) as the explanatory variables:

$$\log\left(Yield_{i,t}\right) = \gamma_1 t + \gamma_2 Tsa_{i,t} + \gamma_3 Prcp_{i,t} + County_i + \varepsilon_{i,t} \quad (3)$$

$\gamma_1 t$ captures the yield increasing trend in recent years. $County_i$ corresponds to fixed effects of county i and accounts for time-invariant county differences, like the soil quality. t stands for each year. $\varepsilon_{i,t}$ stands for the error term for county i at year t. γ_2 or $\frac{\partial \ln(Yield)}{\partial Tsa}$ defines the temperature sensitivity of yield. The temperature sensitivity of BGR (S_T^{BGR}), HI (S_T^{HI}), and GSL (S_T^{GSL}) can be estimated with Equation (3) in a similar way. Here, the dependent variable Yield (BGR, GSL and HI) was logged, so the estimated temperature sensitivity represents the percentage change in Yield (BGR, GSL and HI) with 1°C temperature increase.

The climate data used here were obtained from the University of Idaho Gridded Surface Meteorological Data (http://metdata.northwestknowledge.net/) with a spatial resolution of 4 km (Abatzoglou, 2013). It is a gridded product covering continental United States from 1979 to 2016. This dataset is created by combining the attributes of two datasets: temporally rich data from the North American Land Data Assimilation System Phase 2 (Mitchell, 2004) and spatially rich data from the Parameter-elevation Regressions on Independent Slopes Model (PRISM) (Daly et al., 2008). After validation using an extensive network of weather stations across the United States, this dataset proved to be suitable for application in a landscape-scale ecological model. Then growing season mean Tsa and Prcp were estimated by integrating daily climate variable according to MODIS-derived growing season starting and ending date.

As $Yield = HI \cdot BGR \cdot GSL$, S_T^{Yield} can be written as follows:

$$\frac{\partial \ln(Yield)}{\partial Tsa} = \frac{\partial \ln(HI)}{\partial Tsa} + \frac{\partial \ln(BGR)}{\partial Tsa} + \frac{\partial \ln(GSL)}{\partial Tsa} \quad (4)$$

$$\frac{\partial Yield}{Yield \cdot \partial Tsa} = \frac{\partial HI}{HI \cdot \partial Tsa} + \frac{\partial BGR}{BGR \cdot \partial Tsa} + \frac{\partial GSL}{GSL \cdot \partial Tsa} \quad (5)$$

These equations indicate that the percentage change in yield with 1°C warming can be dissected into percentage changes in BGR, GSL, and HI, which corresponds to physiological processes of carbon assimilation rate through photosynthesis, crop development rate, and maize reproductive growth determining biomass partitioning, respectively. We further divided the dataset of yield, BGR, GSL, and HI into five groups according to the quintile of mean growing season temperature. This separation helps us to understand how maize physiological processes respond to warming as temperature increases.

Although the coefficient in a linear model is easy to interpret, the actual response of crop yield and associated physiological processes

to climate variables is more likely to be nonlinear (Rezaei et al., 2015; Schlenker & Roberts, 2009). Therefore, an alternative model (6) was used by adding a quadratic function of Tsa and Prcp to capture the nonlinear climatic response of yield formation:

$$\log\left(Yield_{i,t}\right)=\gamma_1 t+\gamma_2 Tsa_{i,t}+\gamma_3 Tsa_{i,t}^2+\gamma_4 Prcp_{i,t}+\gamma_5 Prcp_{i,t}^2+County_i+\varepsilon_{i,t} \quad (6)$$

The sensitivity of HI, GSL, and BGR can be modeled similarly by replacing Yield with the corresponding variables.

The total temperature sensitivity of yield estimated above can be regarded as the integrated effects of high temperature stress and thermal time accumulation during different phenological stages. Following previous studies (Schlenker & Roberts, 2009; Tack et al., 2015), yield sensitivity was expressed as:

$$\frac{\partial Yield}{\partial Tsa}=\frac{\partial Yield}{\partial HDD}\frac{\partial HDD}{\partial Tsa}+\frac{\partial Yield}{\partial GDD}\frac{\partial GDD}{\partial Tsa}=\sum_{s=1}^{3}\frac{\partial Yield}{\partial HDD^s}\frac{\partial HDD^s}{\partial Tsa}+\frac{\partial Yield}{\partial GDD^s}\frac{\partial GDD^s}{\partial Tsa} \quad (7)$$

Here high temperature stress is quantified with high temperature degree days (HDD), which characterizes the higher-than-optimal thermal time accumulation. Growing degree days (GDD) drives crop development and characterizes the thermal time accumulation in the absence of extreme conditions. *s* stands for the three growth stages VP, An, and GFP. Based on Equation (7), warming effects on yield through HDD in GFP can be estimated as $\frac{\partial Yield}{\partial HDD^{GFP}}\frac{\partial HDD^{GFP}}{\partial Tsa}$.

When daily maximum temperatures exceed 30 degree, maize kernel set was shown to be reduced by 1.7% per degree day under rainfed conditions in Africa (Lobell, Bänziger, Magorokosho, & Vivek, 2011). Here we also used 30 degree as the threshold to estimate HDD to characterize high temperature stress. GDD and HDD were estimated with the following equations using hourly temperature values, which were obtained by fitting a sine function to interpolate daily maximum Tsa and minimum Tsa.

$$GDD_8^{30}=\sum_{t=1}^{N}DD_t, DD_t=\begin{cases}0, when\ \ Tsa<8\\ Tsa-8, when\ \ 8\le Tsa<30\\ 22, when\ \ Tsa\ge 30\end{cases} \quad (8)$$

$$HDD_{30}^{\infty}=\sum_{t=1}^{N}DD_t, DD_t=\begin{cases}0, when\ Tsa<30\\ Tsa-30, when\ Tsa\ge 30\end{cases} \quad (9)$$

where *t* represents the hourly time step, *N* is the total number of hours in each growing period, and DD is degree days. It has been proved that interpolating daily temperature to hourly value is better in capturing sub-daily heat stress (Tack et al., 2015).

The selected three periods are generally distinguished by their main roles in determining the final yield: vegetative period is related to leaf development and expansion, anthesis is related to pollination and determines grain number, and GFP is related to photosynthate translocation to kernels and determines grain weight. Maize growth stage information is retrieved from the previous study (Zhu et al., 2018). VP is defined as the duration from emergence to 10 days ahead of silking. GFP is defined as the duration from 10 days after silking to maturity. Although we did not exactly extract anthesis timing from the remote sensing data, a previous study suggests that the anthesis is around 1 week before silking (Bolanos & Edmeades, 1996). Hence, in this study, we use 10 days before and after silking date as a conservative estimation of anthesis.

To obtain the sensitivity of maize yield to GDD and HDD in different growth stages, the following panel model was used following previous studies (Schlenker & Roberts, 2009; Tack et al., 2015):

$$Yield_{i,t}=\alpha_0 t+\alpha_1 GDD_{i,t}^{VP}+\alpha_2 HDD_{i,t}^{VP}+\alpha_3 GDD_{i,t}^{An}+\alpha_4 HDD_{i,t}^{An}+\alpha_5 GDD_{i,t}^{GFP}+\alpha_6 HDD_{i,t}^{GFP}+\alpha_7 Prcp_{i,t}+County_i+\varepsilon_{i,t} \quad (10)$$

where $\alpha_0 t$ captures the yield increasing trend, $County_i$ corresponds to the county fixed effects, and $\alpha_1-\alpha_6$ defines the sensitivity of yield to GDD and HDD in the three growth stages. Thus, yield sensitivity to HDD can be estimated with the first-order difference:

$$\alpha_2=\frac{\partial Yield}{\partial HDD^{VP}};\alpha_4=\frac{\partial Yield}{\partial HDD^{An}};\alpha_6=\frac{\partial Yield}{\partial HDD^{GFP}} \quad (11)$$

In terms of the sensitivity of HDD to warming in VP $\left(\frac{\partial HDD^{VP}}{\partial Tsa}\right)$, anthesis $\left(\frac{\partial HDD^{An}}{\partial Tsa}\right)$, and GFP $\left(\frac{\partial HDD^{GFP}}{\partial Tsa}\right)$, daily temperature was uniformly increased by 1°C or 2°C for each stage and then the difference between HDD under warming scenario and the original HDD was used as the sensitivity of HDD to warming. Finally, warming effects on yield through high temperature stress (HDD) in different growth stages can be estimated with the corresponding terms in Equation (7).

2.4 | Relative contribution of heat and water stress to yield decline

Warming trends not only increase the frequency of extreme heat events but also WS by regulating both water demand and water supply (Lobell et al., 2013). Thus the warming influence on yield can be interpreted as the joint effect of high temperature stress (HDD) and WS with the following equation:

$$\frac{\partial Yield}{\partial Tsa}=\frac{\partial Yield}{\partial HDD}\frac{\partial HDD}{\partial Tsa}+\frac{\partial Yield}{\partial GDD}\frac{\partial GDD}{\partial Tsa}+\frac{\partial Yield}{\partial WS}\frac{\partial WS}{\partial Tsa} \quad (12)$$

HDD, GDD, and WS were integrated over the whole growing season.

Sensitivity of HDD, GDD, and WS to temperature $\left(\frac{\partial HDD}{\partial Tsa},\frac{\partial GDD}{\partial Tsa},\frac{\partial WS}{\partial Tsa}\right)$ was estimated with simple linear model through regressing county-level HDD (GDD, WS) over temperature.

To estimate the yield sensitivity to HDD, GDD, and WS, we construct a panel model to regress yield over HDD, GDD and WS:

$$Yield_{i,t}=\beta_0 t+\beta_1 GDD_{i,t}+\beta_2 HDD_{i,t}+\beta_3 WS_{i,t}+County_i+\varepsilon_{i,t} \quad (13)$$

where $\beta_0 t$ captures the linear increasing trend of yield and $County_i$ corresponds to the county fixed effects. Then,

$$\beta_1 = \frac{\partial Yield}{\partial GDD}, \beta_2 = \frac{\partial Yield}{\partial HDD}, \beta_3 = \frac{\partial Yield}{\partial WS} \quad (14)$$

Warming effects on yield through high temperature stress and WS can be thus separately estimated as $\beta_2 \frac{\partial HDD}{\partial Tsa}$ and $\beta_3 \frac{\partial WS}{\partial Tsa}$.

Here, WS was characterized by the ratio of potential evapotranspiration (PET) to evapotranspiration (ET). ET and PET from 2001 to 2015 based on MODIS ET product (MOD16) were employed. This product has a spatial resolution of 1 km with 8-day temporal resolution. ET and PET in MOD16 were estimated using the improved ET algorithm based on the Penman–Monteith equation with MODIS-derived land surface temperature, vegetation cover, and global meteorology data (Mu, Zhao, & Running, 2011). Although various metrics have been proposed to measure WS (Jin et al., 2016), there is no consensus on which one is the best. So far, this observational data-generated ET product is the only one with fine spatial and temporal resolution. MODIS-based growing season PET/ET was calculated for pixels with 70% area covered by maize cropland and then averaged to county level to be consistent with the other variables.

2.5 | Uncertainty quantification

Our sensitivity analysis depends on yield statistical data, satellite-derived phenological date, and vegetation indexes. All of these variables are subject to uncertainties: (1) uncertainties in the county yield statistical data and satellite-derived GSL, IWDRVI; (2) uncertainties of parameters in the regression model converting IWDRVI to AGB. Here we quantified the uncertainties rooted in these datasets through running the panel model for thousands times with the samples generated from a given parameter's confidence interval.

We estimated each county's yield uncertainty based on field level yield data published in a previous study (Lobell et al., 2014), where each county includes 100 samples of yield reports. This dataset enables us to use 1,000 times bootstrap to estimate the standard error (*SE*) of yield in each county. The normalized *SE* (*SE*/mean) is shown in Figure S1. As the field data end in 2012 and we found 92% normalized *SE* during 2000–2012 were smaller than 10%, we set the normalized *SE* during 2013–2015 as 10%, which will be a conservative estimation of yield associated uncertainty. As to the uncertainty related to GSL, we similarly estimated its *SE* through 1,000 times bootstrap based on MODIS-derived pixel level maize GSL information within each county (Figure S2). In terms of BGR and HI, we used the following equations to estimate the associated uncertainty.

$$BGR = \frac{AGB}{GSL} = \frac{\alpha IWDRVI^{\beta}}{GSL} \quad (15)$$

$$HI = \frac{Yield}{AGB} = \frac{Yield}{\alpha IWDRVI^{\beta}} \quad (16)$$

$$Var(BGR) = \left(\frac{\partial BGR}{\partial \alpha}\right)^2 Var(\alpha) + \left(\frac{\partial BGR}{\partial \beta}\right)^2 Var(\beta) + \left(\frac{\partial BGR}{\partial IWDRVI}\right)^2 Var(IWDRVI) + \left(\frac{\partial BGR}{\partial GSL}\right)^2 Var(GSL) \quad (17)$$

$$Var(HI) = \left(\frac{\partial HI}{\partial \alpha}\right)^2 Var(\alpha) + \left(\frac{\partial HI}{\partial \beta}\right)^2 Var(\beta) + \left(\frac{\partial HI}{\partial IWDRVI}\right)^2 Var(IWDRVI) + \left(\frac{\partial HI}{\partial Yield}\right)^2 Var(Yield) \quad (18)$$

The normalized *SE* (*SE*/mean) for BGR and HI is shown in Figures S9 and S10.

With the estimated *SE* for each variable corresponding to each county-year, 1,000 random samples were generated within its 95% confidence interval (mean $\pm$ 1.96 $*$ SE). Therefore, we run the panel model (Equations 3, 10, and 13) 1,000 times with each sample set. The mean of panel model-reported temperature sensitivity confidence interval was used to quantify the uncertainty related to the data source.

2.6 | Crop model output

Here, nine global gridded crop model simulations at 0.5° × 0.5° resolution were selected based on whether maize yield, total biomass, and growing season duration were submitted. These simulations resulted from the joint effort of the Agricultural Model Intercomparison and Improvement Project (AgMIP) (Rosenzweig et al., 2013) and Inter-Sectoral Impact Model Intercomparison Project 1 (ISIMIP1) (Warszawski et al., 2014) for assessing the impact of climate change and management practices on global staple crop production. We selected rainfed maize simulation forced by WFDEI.CRU, as this forcing data covered the longest simulation until 2012. In terms of the management scenario, "harmnon" was selected, meaning the simulation using harmonized fertilizer inputs and assumptions on growing seasons. More details on the simulation protocol could be found in Elliott et al. (2015) and the dataset is described. Then the daily climate data (temperature and precipitation) were integrated over the growing season to estimate the temperature sensitivity of yield, BGR, HI, and GSL with model outputs.

The nine crop models used here can be basically divided into two groups: (a) designed solely for agricultural systems, like pAPSIM, pDSSAT, pDSSAT-pt (pDSSAT-pt is pDSSAT model with the Priestley–Taylor method estimating potential ET), GEPIC, PEGASUS, and CGMS-WOFOST (b) evolving from the terrestrial ecosystem model and covering both natural and agro ecosystems, like CLM-Crop, LPJ-GUESS, and LPJmL. Models in the first group often have a more detailed representation of crop development processes and have a different parameterization of high temperature stress over crop vegetative and reproductive stages. More details on how temperature stress was implemented in the nine crop models can be found in Table S2.

We then applied the abovementioned statistical models to 0.5 × 0.5 gridded AgMIP outputs to investigate (a) how warmer climates influence maize yield through different processes related to BGR, GSL, and HI; and (b) the relative contribution of high temperature stress (characterized with HDD) and WS to maize yield in crop models. We employed model output ET, yield, and estimated PET using the Penman–Monteith equation forced by WFDEI.CRU as well.

2.7 | APSIM model experiment

The APSIM model is a process-based crop model that explicitly accounts for the high temperature stress and WS during different crop growth stages, which is also included in ISIMIP1 (pAPSIM, the parallel version APSIM). It simulates a number of crops under various climatic and management conditions, and hence is used worldwide to address various research questions related to agricultural systems (Holzworth et al., 2014). The APSIM-Maize module is inherited from the CERESMaize, with modifications on stress representation, biomass growth rate, and phenological development. This flexible process-based model allows us to investigate the different roles of high temperature stress across stages in determining maize yield variation.

Water stress in APSIM is calculated as the ratio of water supply to water demand. Water demand is driven by the potential biomass growth rate and transpiration efficiency that is adjusted for vapor pressure deficit (VPD). Water supply is calculated as the amount of water above the crop's wilting point in soil layers containing roots. This amount is multiplied by a KL factor that accounts for the ability of roots to extract water from a soil layer. As temperature rises, it will increase water demand through VPD and will reduce the supply of soil water through elevated ET.

Here, we designed two grid-based simulation experiments to further investigate how WS and high temperature stress influence maize yield with increasing temperature: sim1 is a control simulation using default temperature stress and WS; sim2 is a simulation with temperature stress blocked. More details on model setup can be found in the Supplementary Information. Here we only block high temperature stress, because WS is more complex to manipulate. Sim1 includes both high temperature stress and WS during photosynthesis, anthesis, and grain filling, whereas sim2 only includes WS. Thus, high temperature stress can be separately estimated by comparing the two simulation outputs. The simulation is run for the three states over 2000–2015 and forced with University of Idaho Gridded Surface Meteorological Data as well. Soil parameters, such as soil hydraulic properties and soil organic matter fractions, were extracted from the State Soil Geographic (STATSGO) database, as collected by the National Cooperative Soil Survey over the course of a century. For each simulation grid, the soil information was obtained through the R package "soil DB" (http://ncss-tech.github.io/AQP/). Management information like planting density and fertilizer application amount was taken from the USDA NASS survey report at the state level. Crop sowing date was derived from the Crop Calendar Dataset (Sacks, Deryng, Foley, & Ramankutty, 2010). The generic maize hybrid ("B_110") included in APSIM version 7.7 was used and it refers to a hybrid with a 110-day relative maturity. The phenology-related parameters characterizing GFP thermal time requirement were spatially parameterized based on MODIS-derived crop stage information (Zhu et al., 2018). Spatially explicit parameters are expected to improve model simulation with a better match with the actual maize phenological development.

3 | RESULTS

According to the regression model (Figure 1), spatially explicit AGB was estimated with MODIS-derived IWDRVI. BGR, GSL, and HI at county level were also retrieved. Their multi-year mean reveals there is a clear variation in the spatial pattern of BGR, HI, and yield, and lower values are often identified in those southern counties (Figure 2). However, GSL is relatively homogeneous across the counties, implying varieties with different maturity groups were selected to adapt to the local thermal time environment. Thus the correlation between GSL and yield is quite low (R^2 = 0.004), but this does not contradict the fact that longer GSL leads to higher yield for a given site. The spatial variation of yield is more correlated with HI (R^2 = 0.88) and BGR (R^2 = 0.74), implying the dominant role of daily biomass accumulation and partitioning to grain in driving the yield variation spatially.

S_T^{Yield} was estimated and then decomposed into three components: S_T^{BGR}, S_T^{HI}, and S_T^{GSL} with Equation (5). Each component represents different physiological controls of temperature on maize yield through reproductive growth during anthesis and GFP (S_T^{HI}), photosynthesis dominated carbon assimilation (S_T^{BGR}), and plant development rate (S_T^{GSL}). Although S_T^{Yield} varies considerably among individual crop models, a similar estimation of S_T^{Yield} is identified between the model ensemble mean (MEM, −7.1 ± 3.1% per °C) and observations (−7.2 ± 0.9% per °C) (Figure 3). When we looked into each component, MEM overestimated S_T^{GSL} while underestimated S_T^{HI} compared with the corresponding estimation based on observational evidence. As model parameters are normally based on the knowledge of crop development and growth processes late 20th century, this discrepancy probably suggests that the development rate of newly adopted maize cultivar might have better adapted to warmer climate while little progress has been achieved for dealing with warming effects during maize reproductive growth. Instead, management practices intended to improve yield, such as higher application of nitrogen fertilizer, might lead to higher sensitivity of heat stress during grain formation processes (Ordóñez, Savin, Cossani, & Slafer, 2015; Wahid, Gelani, Ashraf, & Foolad, 2007). In terms of the sensitivity of BGR, both MEM and data show a weak response, consistent with the fact that maize photosynthesis has a relatively high optimal temperature (Dekov, Tsonev, & Yordanov, 2000). Some models, like LPJ-GUESS, overestimated the warming influence on BGR but underestimated the influence on HI, which suggests that in these models, excessive temperature stress is imposed on processes related to photosynthesis while the stress during grain formation is overlooked.

The temperature sensitivity analysis was further divided into five groups based on the quintile of growing season mean temperature, which provides an insight into how temperature sensitivity evolves as the mean temperature increases in the future. Generally, S_T^{Yield} estimated with observational evidence is significantly enhanced in warmer divisions, which changes from 0.3 ± 1.1% per degree Celsius to −16.6 ± 4.3% per degree Celsius from the lowest to highest temperature quintile (Figure 4a). It is noted that the increase in S_T^{Yield} is mainly driven by S_T^{HI}, which varies from 1.5 ± 1.4% per degree Celsisu

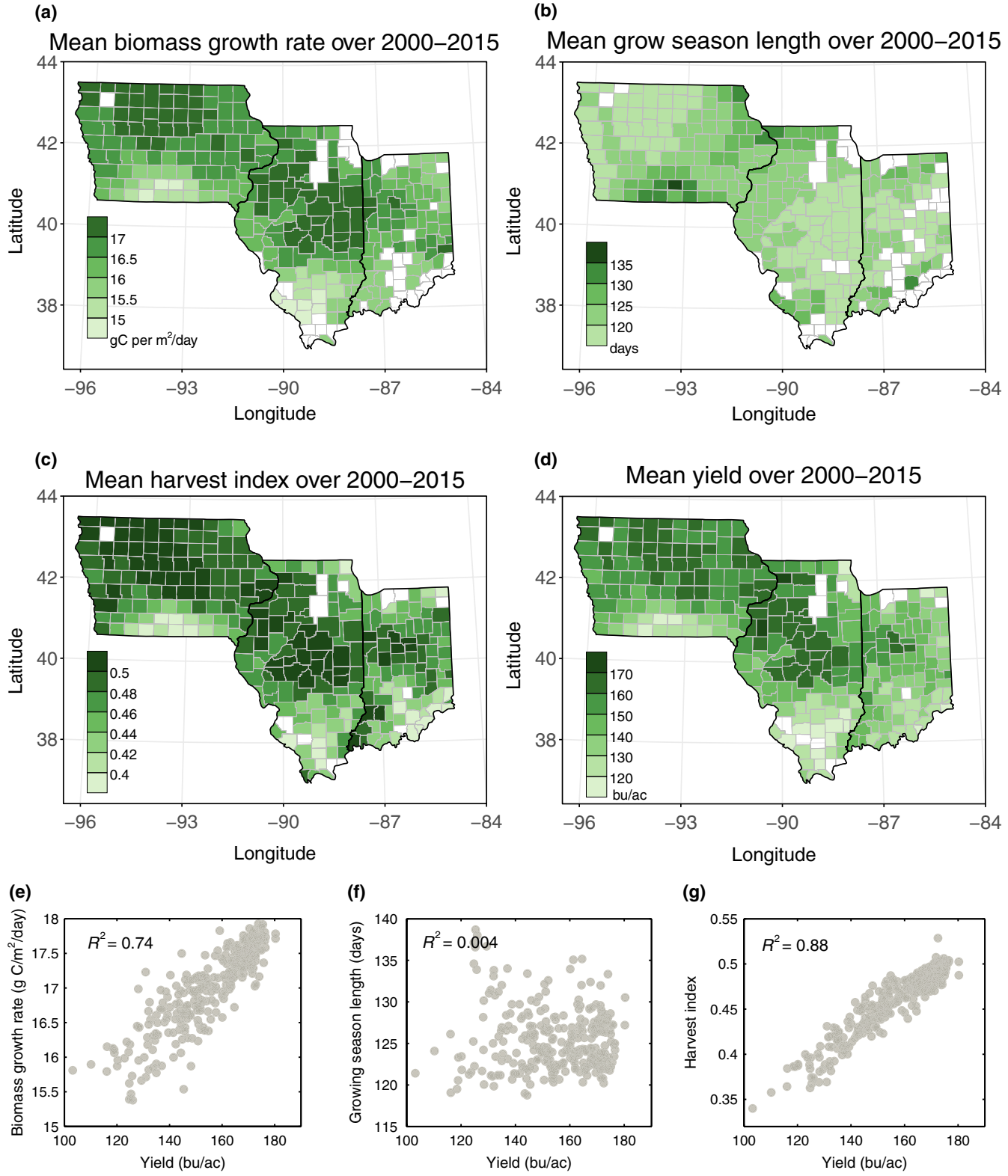

FIGURE 2 Spatial pattern of multi-year mean biomass growth rate (BGR), growing season length (GSL), harvest index (HI), and Yield at county level over 2000–2015 across the three Midwest states (a–d). Correlation between yield and multi-year mean BGR, GSL, and HI with each point representing a county (e–g). The correlation analysis suggests that yield variation is spatially correlated with HI and BGR but not GSL

to –12.6 ± 3.8% per degree Celsius, correspondingly. This result confirms the conclusion based on field experiments that warming during grain formation is more influential (Edreira & Otegui, 2012; Siebers et al., 2017). Despite increasing background temperature, S_T^{GSL} keeps a relatively stable value of approximately –2.6% per degree Celsius and S_T^{BGR} shows a small enhancement. Therefore, it can be inferred

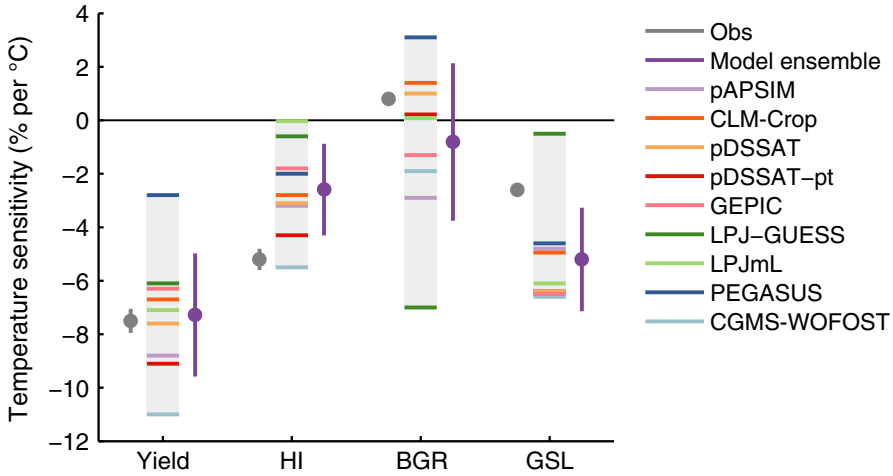

FIGURE 3 Temperature sensitivity of yield, harvest index (HI), biomass growth rate (BGR), and growing season length (GSL) based on satellite data and National Agricultural Statistics Service -reported yield (grey vertical line) and crop models, where the horizontal color lines within the shaded area indicate sensitivity estimation in each model and vertical purple lines indicate model ensemble estimation. The error bars represent the 95% confidence interval of estimated sensitivity. The observational data-based temperature sensitivity uncertainties were estimated through resampling. The mean sensitivity and confidence interval for MEM and observational data are also reported in Table S3. This figure suggests that yield sensitivity is mainly driven by HI, but model ensemble overestimated effects through GSL

that warming-induced yield decline is mainly driven by GSL in the three lower temperature divisions, whereas the effects of warming on HI become more dominant in the two higher temperature divisions (Figure 4a).

When model output was similarly divided based on the quintile of growing season mean temperature, MEM of S_T^{Yield}, S_T^{BGR}, S_T^{GSL}, and S_T^{HI} was used to gain insight into how warming effects were represented in crop models. The individual model performance is shown in Figure S6. Compared with the estimations with observational data, MEM reproduces the patterns of S_T^{Yield}, S_T^{BGR}, S_T^{GSL}, and S_T^{HI} across the temperature gradient (Figure 4b). Changes in MEM S_T^{HI} drive the increasing S_T^{Yield} (Figure 4b), but S_T^{HI} is underestimated relative to observational data. In terms of S_T^{GSL}, it is overestimated for all five temperature quintiles (approximately –5.4% per degree Celsius relative to –2.6% per degree Celsius in observational data estimation). The stable S_T^{GSL} estimated with both crop models and observational data suggests that maize plant development is quasi-linearly driven by temperature (Edreira & Otegui, 2012; Hatfield & Prueger, 2015)

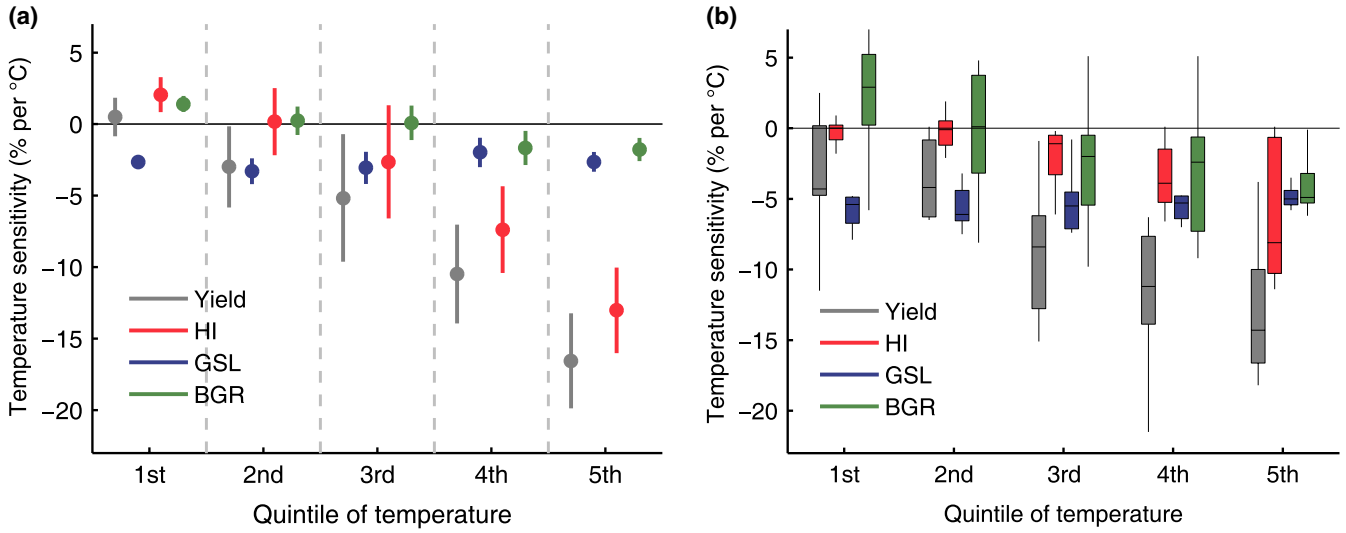

FIGURE 4 Temperature sensitivity of yield, harvest index (HI), biomass growth rate (BGR), and growing season length (GSL) when yield, HI, BGR, and GSL were divided by the quintile of growing season mean temperature based on satellite data and National Agricultural Statistics Service yield (a) and based on crop models (b). The error bars in (a) represent the 95% confidence interval of estimated sensitivity. Boxplots in (b) indicate the median (horizontal line), 25th–75th percentile (gray box), and 5th–95th percentile (whiskers) of crop model-estimated temperature sensitivity. This figure suggests that the nonlinear response of yield sensitivity is mainly driven by HI. Although the model ensemble shows a similar pattern, it overestimated effects through GSL

and is relatively more heat tolerant compared with wheat plants, which show an accelerated senescence when exposed to heat stress (Lobell et al., 2012). The small enhancement in S_T^{BGR} estimated with both crop model and observational data suggests that photosynthesis-dominated BGR is likely to be slightly influenced under future warmer climate, which might result from the higher optimal temperature of C_4 photosynthesis.

We also used an alternative panel model (Equation 6) by adding quadratic function of Tsa and Prcp to capture the nonlinear response of yield, HI, BGR, and GSL to climate variation. The temperature response of yield, HI, BGR, and GSL was expressed as the normalized quadratic function of temperature. This alternative analysis demonstrated that as temperature rises, the nonlinear response of yield is mainly driven by HI while yield decline through GSL is linear, which is in line with the statistical analysis using grouped temperature gradient (Figure 5). The temperature response curves also confirm that the optimal temperature of BGR is higher than that of HI and yield (Edreira & Otegui, 2012).

As the nonlinear reduction of yield and HI by warming remains unclear, a panel data model was used to investigate the different sensitivity of yield to HDD during vegetative period $\left(\frac{\partial Yield}{\partial HDD^{VP}}\right)$, anthesis $\left(\frac{\partial Yield}{\partial HDD^{An}}\right)$, and GFP $\left(\frac{\partial Yield}{\partial HDD^{GFP}}\right)$. The analysis suggests that yield is the most sensitive to HDD during GFP (–0.46 ± 0.07% per degree days) (Figure 6a), which is in line with field heating experiments (Edreira, Mayer, & Otegui, 2014; Ruiz-Vera et al., 2018; Siebers et al., 2017). The yield sensitivity to HDD during anthesis (–0.33 ±0.11% per degree days) is slightly higher than HDD during VP (–0.30 ± 0.12% per degree days) (Figure 6a). The yield sensitivity to GDD is small in all three periods and even shows a positive response for GDD in VP and GFP (Figure 6a). Meanwhile, the increase in HDD during GFP is the largest of the three stages, probably due to the high background temperature (Figure 6b). According to Equation (7), when a uniform 1°C and 2°C warming is applied to whole growing season temperature, yield is reduced by 5.9% and 21.7%, respectively. When 1°C (2°C) warming was separately applied to HDD during "VP," "Anthesis," and "GFP," maize yield will be reduced by 1.8% (6.9%), 1.3% (5.2%), and 3.3% (13.1%), respectively (Figure 6c). This nonuniform response suggests that the warming-induced higher HDD during GFP exclusively accounted for more than half of yield reduction and was the main driver of yield decline.

In addition to direct heat stress, it was previously suggested that an extreme heat event might threaten maize yield indirectly through

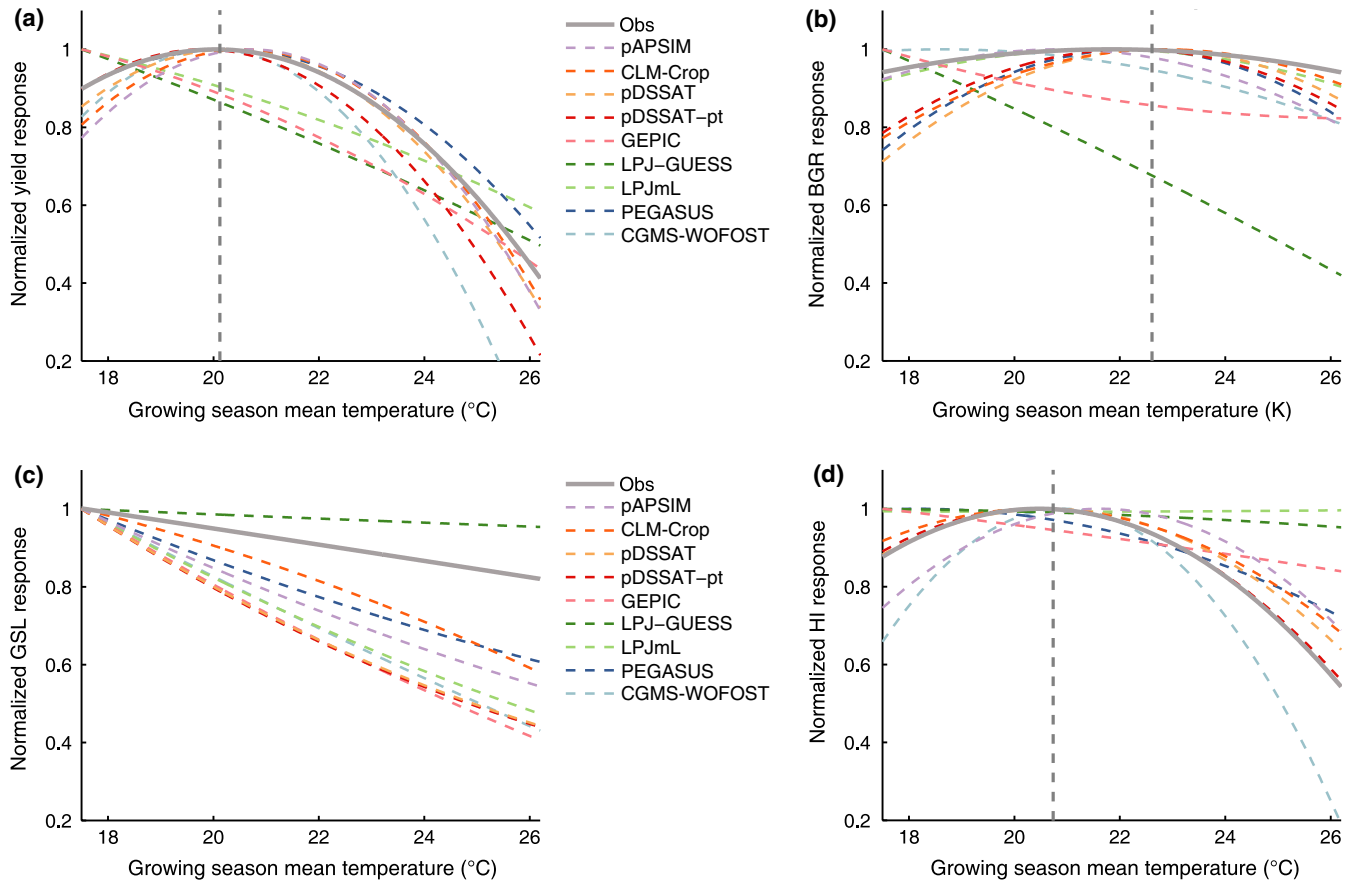

FIGURE 5 Response of Yield (a), biomass growth rate (BGR) (b), growing season length (GSL) (c), and harvest index (HI) (d) to growing season mean temperature. The vertical dashed lines indicate the optimal mean temperature of Yield, HI, or BGR derived from observational evidence. The response function is normalized by the maximum value in each response. The X-axis range is determined by the minimum and maximum mean growing season temperature across the U.S. Midwest during 2000–2015. The confidence interval of temperature response curve for each model results is also reported in Figure S8

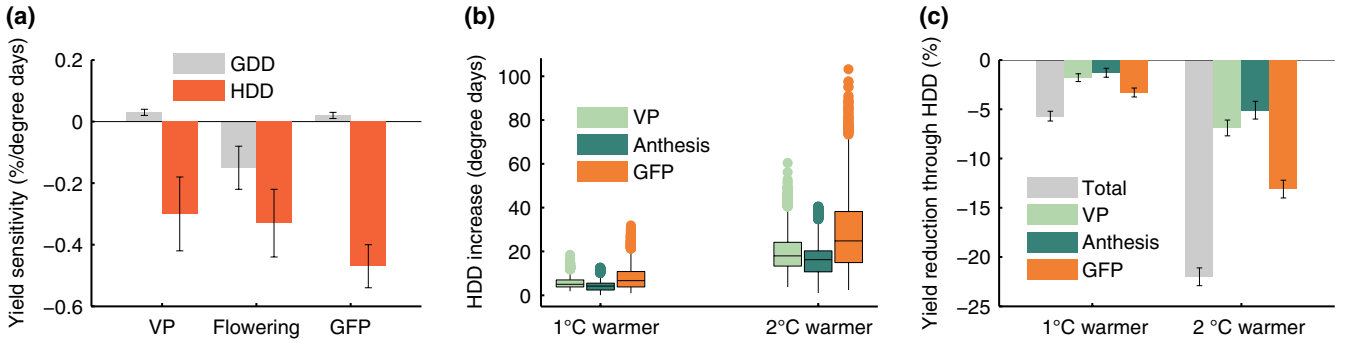

FIGURE 6 Sensitivity of maize yield based on National Agricultural Statistics Service report to growing degree days (GDD) and high temperature degree days (HDD) in different growing stages: vegetative period (VP), anthesis, and grain filling period (GFP) (a). Boxplot of HDD increase in response to 1°C and 2°C warming (b). Boxplots indicate the median, 25–75th percentile, and 5th–95th percentile of HDD increase across all counties during 2000–2015. Estimation of yield reduction is based on to the regression model (Equation 7). Yield reduction of "All season" indicates the temperature was increased uniformly across the whole growing season, whereas "VP," "Anthesis," and "GFP" means temperature was increased exclusively for HDD during "VP," "Anthesis," and "GFP." The yield reduction here characterizes the relative contribution of high temperature stress during a specific maize stage. Error bars in (a) and (c) represent the 95% confidence interval of estimated sensitivity through resampling, which are also reported in Tables S4 and S5

WS (Lobell et al., 2013). A better discernment of the effect of WS and heat stress would help farmers to make proper decisions to better adapt to future warming challenges. A panel model analysis was used here to estimate the relative contribution of WS (PET/ET) and high temperature stress (HDD) on yield. The model result suggests that 1°C warming will increase GDD, HDD, and WS by 50 ± 3.3 degree days, 17 ± 1.2 degree days, and $0.011 \pm 8 \times 10^{-4}$, respectively (Figure 7a). However, a unit increase in GDD, HDD, and WS causes yield decline of –0.0054 ± 0.001%, –0.27 ± 0.04%, and –1.54 ± 0.48%, respectively (Figure 7a). Taken together, the regression model shows that 1°C warming will reduce yield by 0.2 7± 0.15%, 4.6 ± 1.0%, and 1.7 ± 0.65% through GDD, HDD, and WS, respectively (Figure 7a), suggesting that the warmer temperature reduces maize yield mainly through direct high temperature stress. The mean sensitivity and confidence interval is also reported in Table S4.

When the same panel model was applied to crop model output from AgMIP, the model results generally showed small warming effects through GDD but varied substantially in terms of the warming effects through WS and HDD. Compared with the observational evidence, MEM underestimated the direct high temperature influence through HDD but overestimated the indirect influence through WS (Figure 7b). As suggested in a field CO_2 enrichment experiment on maize, water conservation effects of increasing CO_2 might result in more yield benefit under WS conditions (Hussain et al., 2013; Jin et al., 2017) but its yield benefit under heat stress may be limited (Siebers et al., 2015). This implies that in current crop models the direct high temperature stress on yield is underestimated, whereas the yield benefit of elevated atmospheric CO_2 is overestimated. This discrepancy could bias the projection of maize yield variation given future higher atmospheric CO_2 and more frequent heat waves.

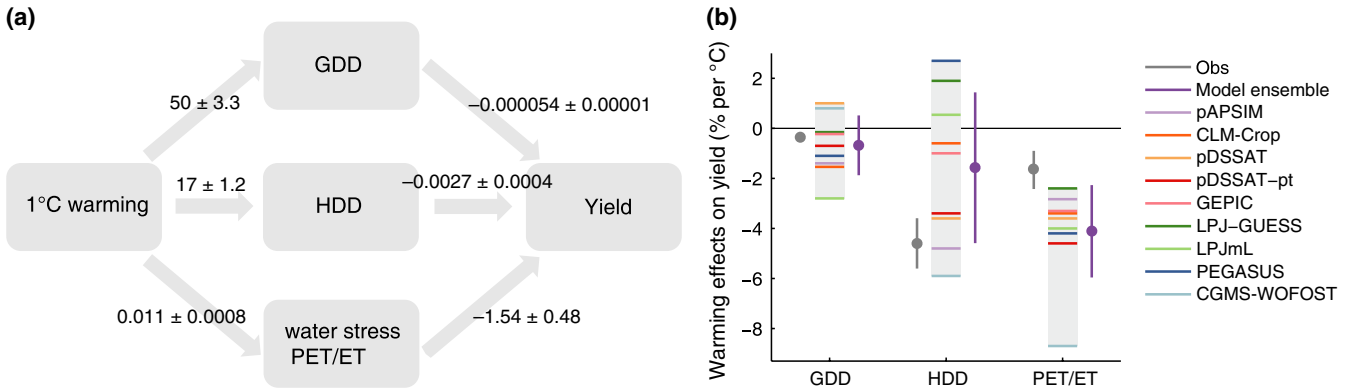

FIGURE 7 The effect of warming-induced direct heat (HDD) and indirect water stress (WS) on maize yield based on National Agricultural Statistics Service yield report, MODIS-derived crop stages information, and MODIS PET/ET product (MOD16) (a). The numbers marked on the arrows indicate the effects of 1°C warming on yield through growing degree days (GDD), high temperature degree days (HDD), and water stress (WS), corresponding to the coefficients in Equation (12). Comparison of warming effects on maize yield through GDD, HDD, and WS (potential evapotranspiration [PET]/evapotranspiration [ET]) estimated from observational evidence and crop models (b). Error bars for observational data represent the 95% confidence interval through sampling (details in Table S6) and error bars in model ensemble represent the stand deviation of multi-model estimated yield responses (b)

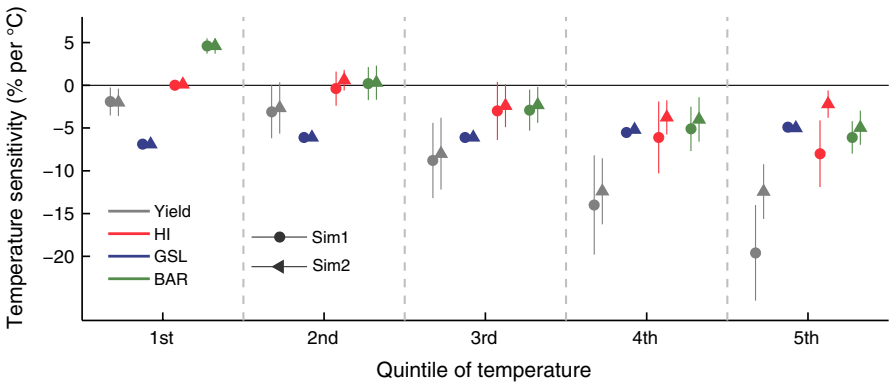

FIGURE 8 Temperature sensitivity of yield, harvest index (HI), growing season length (GSL), and daily biomass growth rate (BGR) divided by quintile of growing season mean temperature in two APSIM simulation results. sim1 (circle) is the simulation with both water and high temperature stress and sim2 (triangle) is the simulation with only water stress

Although the MEM suggests a lower influence of temperature through HDD, there are individual models with close estimation to observational data. For example, the APSIM crop model suggests a higher influence of temperature through HDD than through WS (Figure 7b). We also applied the APSIM model default WS metric, the ratio of water supply to water demand, as the WS term to construct an alternative panel model to test whether the results are robust to the selection of WS metric. This alternative metric produced a similar estimation of warming effects on yield through GDD, HDD, and WS as the one using PET/ET as the WS metric (Figure S4).

A model experiment was designed to better understand how WS and heat stress influence maize yield through different physiological processes. In this experiment, sim1 is the control run with both high temperature stress and WS, whereas sim2 blocked the high temperature stress. The results show that as temperature increases, there is no significant change in S_T^{BGR} and S_T^{GSL} between sim1 and sim2 but S_T^{HI} is significantly enhanced in sim2 (Figure 8). As GSL is mainly driven by thermal time accumulation, S_T^{GSL} shows a similar response with increasing background temperature in both sim1 and sim2. Thus, the other two components S_T^{BGR} and S_T^{HI} represent the main effects of high temperature stress on yield. The comparison between sim1 and sim2 suggests that, as temperature rises, high temperature stress reduces maize yield primarily through process related to grain formation, whereas the high temperature-induced WS influences yield mainly through processes related to BGR, such as photosynthesis or respiration (Figure 8).

4 | DISCUSSION

By integrating satellite observations, crop model simulations, surveys, and experimental data, we examined the response of maize yield and its constituent processes to high temperature stress in an analytical way. The results suggest that the nonlinear response of yield $\left(S_T^{Yield}\right)$ can be decomposed into small effects on S_T^{BGR}, linear $\left(S_T^{GSL}\right)$, and non-linear $\left(S_T^{HI}\right)$ processes, and that heat stress during GFP poses a striking threat for maize yield decline. Photosynthesis-dominated BGR is only marginally influenced by temperature stress, which is likely to result from the higher optimal temperature of C_4 photosynthesis. With the advancement in computing power and finer spatial and spectral information brought with new satellite data, the methodology here can be readily extrapolated to other regions and further improve our understanding of maize and other crop yield performance under extreme conditions.

Our analysis also pinpoints both strengths and weaknesses of crop models in charactering high temperature stress on maize yield and provides an important feedback for the crop modeling community. Most models underestimated the warming effects through HI while overstated the temperature sensitivity of GSL. Meanwhile, the indirect WS effect was overestimated in most crop models, which might bring substantial uncertainties when projecting maize yield under future hotter conditions. One explanation for the discrepancy between estimations based on model and observational datasets is possibly the issue of different scales, since crop models operated at 0.5° × 0.5° grids and observational datasets were analyzed at the county level. However, it is more likely due to the limitation of models in accurately representing heat stress influence, such as slow updates of key parameters related to heat and drought resistance and lack of explicitly accounting for heat stress effect during the development stages of different maize cultivars. Rezaei, Siebert, Hüging, and Ewert (2018) also found that ignoring cultivar changes in analyses of historic changes in phenology leads to an overestimate of the temperature sensitivity of the phenology of winter wheat in Germany. A similar model parametrization bias may exist in other crops, e.g. maize in the United States.

In addition, most evaluated models, except CLM-Crop, lack a canopy energy balance scheme to simulate leaf temperature and therefore use air temperature instead of leaf temperature to parameterize effects of heat stress. However, air temperature can deviate significantly from leaf temperature, especially under dry conditions or elevated CO_2 where canopies can be several degrees hotter than the air due to reduced transpiration. Thus, improvement in canopy energy balance among all models is necessary for better representing the heat stress effects on crop yield (Webber et al., 2017).

The selected metric here to quantify heat stress and WS is also important for evaluating their relative contributions to yield decline. Threshold-based thermal time accumulation has been widely used to characterize heat stress (Deryng, Sacks, Barford, & Ramankutty, 2011; Lobell et al., 2012; Schlenker & Roberts, 2009).

In terms of WS, several metrics have been proposed, such as VPD, PET/ET, soil moisture content, and the ratio of water supply to water demand (Jin et al., 2016; Lobell et al., 2014). Higher VPD means an increase in atmospheric water demand and can decrease photosynthetic activity through reducing stomatal conductance. Soil water content regulates transport of water in the soil–plant–atmosphere continuum and determines the amount of extractable water by crop plants. PET/ET and the ratio of water supply to water demand accounts for both atmospheric water demand and soil water availability. These two metrics also give a similar estimate of WS effects on maize yield (Figure S4). Due to the different roles of VPD and soil water content in determining the plant physiological processes, it might be useful to disentangle the two effects. However, there are limited controlled experiments designed to address the different responses of crop plants to atmospheric water demand (VPD) and soil water dryness, partly because VPD is often hard to be controlled in the field conditions (Gray et al., 2016). In this context, more field experiments are necessary to mechanistically understand the relative contribution of different sources of WS on crop yield.

Overall, our analysis through model-data integration suggests that warming-induced decline in maize yield is mainly driven by direct heat stress imposed on reproductive processes, whereas indirect WS only contributes a small fraction. Therefore, future adaptation strategies should be targeted at the heat stress during grain formation. As model parameterization used here often represents a static management system from around the year 2000 (Elliott et al., 2015), the discrepancy in temperature sensitivity between crop model simulations and observational data suggests that changes in management systems need to be better accounted for to achieve progress in heat stress estimates (Glotter & Elliott, 2016).

ACKNOWLEDGEMENTS

We thank three anonymous reviewers whose comments significantly improved this study. This research was supported by an NSF project (IIS-1027955) and a NASA LCLUC project (NNX09AI26G) to Q. Z. We acknowledge the Rosen High Performance Computing Center at Purdue for computing support.

ORCID

Peng Zhu https://orcid.org/0000-0001-7835-3971
Christoph Müller https://orcid.org/0000-0002-9491-3550

REFERENCES

Abatzoglou, J. T. (2013). Development of gridded surface meteorological data for ecological applications and modelling. *International Journal of Climatology*, *33*, 121–131. https://doi.org/10.1002/joc.3413

Assefa, Y., Prasad, P. V. V., Carter, P., Hinds, M., Bhalla, G., Schon, R., … Ciampitti, I. A. (2017). A new insight into corn yield: Trends from 1987 through 2015. *Crop Science*, *57*(5), 2799–2811. https://doi.org/10.2135/cropsci2017.01.0066

Assefa, Y., Vara Prasad, P. V., Carter, P., Hinds, M., Bhalla, G., Schon, R., … Ciampitti, I. A. (2016). Yield responses to planting density for US modern corn hybrids: A synthesis-analysis. *Crop Science*, *56*, 2802–2817. https://doi.org/10.2135/cropsci2016.04.0215

Asseng, S., Ewert, F., Martre, P., Rötter, R. P., Lobell, D. B., Cammarano, D., … Zhu, Y.. (2014). Rising temperatures reduce global wheat production. *Nature Climate Change*, *5*, 143–147.

Azzari, G., Jain, M., & Lobell, D. B. (2017). Towards fine resolution global maps of crop yields: Testing multiple methods and satellites in three countries. *Remote Sensing of Environment*, *202*, 129–141. https://doi.org/10.1016/j.rse.2017.04.014

Bolanos, J., & Edmeades, G. O. (1996). The importance of the anthesis-silking interval in breeding for drought tolerance in tropical maize. *Field Crops Research*, *48*(1), 65–80. https://doi.org/10.1016/0378-4290(96)00036-6

Butler, E. E., & Huybers, P. (2015). Variations in the sensitivity of US maize yield to extreme temperatures by region and growth phase. *Environmental Research Letters*, *10*(3), 034009.

Cheikh, N. C., & Jones, R. J. (1994). Disruption of kernel growth and development by heat stress: Role of cytokinin/ABA balance. *Plant Physiology*, *106*, 45–51.

Cicchino, M., Rattalino Edreira, J. I., Uribelarrea, M., & Otegui, M. E. (2010). Heat stress in field-grown maize: Response of physiological determinants of grain yield. *Crop Science*, *50*, 1438–1448. https://doi.org/10.2135/cropsci2009.10.0574

Commuri, P. D., & Jones, R. J. (2001). High temperatures during endosperm cell division in maize. *Crop Science*, *41*(4), 1122–1130. https://doi.org/10.2135/cropsci2001.4141122x

Crafts-Brandner, S. J., & Salvucci, M. E. (2002). Sensitivity of photosynthesis in a C4 plant, maize, to heat stress. *Plant Physiology*, *129*(4), 1773–1780.

Daly, C., Halbleib, M., Smith, J. I., Gibson, W. P., Doggett, M. K., Taylor, G. H., … Pasteris, P. P. (2008). Physiographically sensitive mapping of climatological temperature and precipitation across the conterminous United States. *International Journal of Climatology*, *28*(15), 2031–2064. https://doi.org/10.1002/joc.1688

Deines, J. M., Kendall, A. D., & Hyndman, D. W. (2017). Annual irrigation dynamics in the U.S. Northern high plains derived from landsat satellite data. *Geophysical Research Letters*, *44*, 9350–9360. https://doi.org/10.1002/2017GL074071

Dekov, I., Tsonev, T., & Yordanov, I. (2000). Effects of water stress and high-temperature stress on the structure and activity of photosynthetic apparatus of *Zea mays* and *Helianthus annuus*. *Photosynthetica*, *38*, 361–366.

Deryng, D., Sacks, W. J., Barford, C. C., & Ramankutty, N. (2011). Simulating the effects of climate and agricultural management practices on global crop yield. *Global Biogeochemical Cycles*, *25*(2). https://doi.org/10.1029/2009GB003765

Dias, A. S., & Lidon, F. C. (2009). Evaluation of grain filling rate and duration in bread and durum wheat, under heat stress after anthesis. *Journal of Agronomy and Crop Science*, *195*, 137–147.

Edreira, J. I. R., Mayer, L. I., & Otegui, M. E. (2014). Heat stress in temperate and tropical maize hybrids: Kernel growth, water relations and assimilate availability for grain filling. *Field Crops Research*, *166*, 162–172. https://doi.org/10.1016/j.fcr.2014.06.018

Edreira, J. I. R., & Otegui, M. E. (2012). Heat stress in temperate and tropical maize hybrids: Differences in crop growth, biomass partitioning and reserves use. *Field Crops Research*, *130*, 87–98. https://doi.org/10.1016/j.fcr.2012.02.009

Edreira, J. I. R., & Otegui, M. E. (2013). Heat stress in temperate and tropical maize hybrids: A novel approach for assessing sources of kernel loss in field conditions. *Field Crops Research*, *142*, 58–67. https://doi.org/10.1016/j.fcr.2012.11.009

Eitzinger, J., Thaler, S., Schmid, E., Strauss, F., Ferrise, R., Moriondo, M., … Çaylak, O. (2013). Sensitivities of crop models to extreme weather

conditions during flowering period demonstrated for maize and winter wheat in Austria. *Journal of Agricultural Science*, *151*, 813–835. https://doi.org/10.1017/S0021859612000779

Elliott, J., Müller, C., Deryng, D., Chryssanthacopoulos, J., Boote, K. J., Büchner, M., … Sheffield, J. (2015). The Global Gridded Crop Model Intercomparison: Data and modeling protocols for Phase 1 (v1.0). *Geoscientific Model Development*, *8*, 261–277. https://doi.org/10.5194/gmd-8-261-2015

Gitelson, A. A. (2004). Wide dynamic range vegetation index for remote quantification of biophysical characteristics of vegetation. *Journal of Plant Physiology*, *161*, 165–173. https://doi.org/10.1078/0176-1617-01176

Glotter, M., & Elliott, J. (2016). Simulating US agriculture in a modern Dust Bowl drought. *Nature Plants*, *3*(1), 16193.

Gray, S. B., Dermody, O., Klein, S. P., Locke, A. M., McGrath, J. M., Paul, R. E., … Leakey, A. D. B. (2016). Intensifying drought eliminates the expected benefits of elevated carbon dioxide for soybean. *Nature Plants*, *2*(9), 16132. https://doi.org/10.1038/nplants.2016.132

Guan, K., Wu, J., Kimball, J. S., Anderson, M. C., Frolking, S., Li, B. O., … Lobell, D. B. (2017). The shared and unique values of optical, fluorescence, thermal and microwave satellite data for estimating large-scale crop yields. *Remote Sensing of Environment*, *199*, 333–349. https://doi.org/10.1016/j.rse.2017.06.043

Guindin-Garcia, N., Gitelson, A. A., Arkebauer, T. J., Shanahan, J., & Weiss, A. (2012). An evaluation of MODIS 8- and 16-day composite products for monitoring maize green leaf area index. *Agricultural and Forest Meteorology*, *161*, 15–25. https://doi.org/10.1016/j.agrformet.2012.03.012

Hatfield, J. L., & Prueger, J. H. (2015). Temperature extremes: Effect on plant growth and development. *Weather and Climate Extremes*, *10*, 4–10. https://doi.org/10.1016/j.wace.2015.08.001

Holzworth, D. P., Huth, N. I., deVoil, P. G., Zurcher, E. J., Herrmann, N. I., McLean, G., … Keating, B. A. (2014). APSIM – Evolution towards a new generation of agricultural systems simulation. *Environmental Modelling & Software*, *62*, 327–350. https://doi.org/10.1016/j.envsoft.2014.07.009

Hussain, M. Z., VanLoocke, A., Siebers, M. H., Ruiz-Vera, U. M., Cody Markelz, R. J., Leakey, A. D. B., … Bernacchi, C. J. (2013). Future carbon dioxide concentration decreases canopy evapotranspiration and soil water depletion by field-grown maize. *Global Change Biology*, *19*, 1572–1584. https://doi.org/10.1111/gcb.12155

Jin, Z., Zhuang, Q., Tan, Z., Dukes, J. S., Zheng, B., & Melillo, J. M. (2016). Do maize models capture the impacts of heat and drought stresses on yield? Using algorithm ensembles to identify successful approaches. *Global Change Biology*, *22*, 3112–3126. https://doi.org/10.1111/gcb.13376

Jin, Z., Zhuang, Q., Wang, J., Archontoulis, S. V., Zobel, Z., & Kotamarthi, V. R. (2017). The combined and separate impacts of climate extremes on the current and future US rainfed maize and soybean production under elevated CO_2. *Global Change Biology*, *23*, 2687–2704.

Lizaso, J. I., Ruiz-Ramos, M., Rodríguez, L., Gabaldon-Leal, C., Oliveira, J. A., Lorite, I. J., … Rodríguez, A. (2018). Impact of high temperatures in maize: Phenology and yield components. *Field Crops Research*, *216*, 129–140. https://doi.org/10.1016/j.fcr.2017.11.013

Lobell, D. B., Bänziger, M., Magorokosho, C., & Vivek, B. (2011). Nonlinear heat effects on African maize as evidenced by historical yield trials. *Nature Climate Change*, *1*, 42–45. https://doi.org/10.1038/nclimate1043

Lobell, D. B., Hammer, G. L., McLean, G., Messina, C., Roberts, M. J., & Schlenker, W. (2013). The critical role of extreme heat for maize production in the United States. *Nature Climate Change*, *3*(5), 497–501. https://doi.org/10.1038/nclimate1832

Lobell, D. B., Roberts, M. J., Schlenker, W., Braun, N., Little, B. B., Rejesus, R. M., & Hammer, G. L. (2014). Greater sensitivity to drought accompanies maize yield increase in the U.S. Midwest. *Science*, *344*, 516–519. https://doi.org/10.1126/science.1251423

Lobell, D. B., Sibley, A., & Ivan Ortiz-Monasterio, J. (2012). Extreme heat effects on wheat senescence in India. *Nature Climate Change*, *2*, 186–189. https://doi.org/10.1038/nclimate1356

Lobell, D. B., Thau, D., Seifert, C., Engle, E., & Little, B. (2015). A scalable satellite-based crop yield mapper. *Remote Sensing of Environment*, *164*, 324–333. https://doi.org/10.1016/j.rse.2015.04.021

Mazdiyasni, O., & AghaKouchak, A. (2015). Substantial increase in concurrent droughts and heatwaves in the United States. *Proceedings of the National Academy of Sciences*, *112*, 11484–11489.

Mitchell, K. E. (2004). The multi-institution North American Land Data Assimilation System (NLDAS): Utilizing multiple GCIP products and partners in a continental distributed hydrological modeling system. *Journal of Geophysical Research*, *109*, D07S90. https://doi.org/10.1029/2003JD003823

Mu, Q., Zhao, M., & Running, S. W. (2011). Improvements to a MODIS global terrestrial evapotranspiration algorithm. *Remote Sensing of Environment*, *115*(8), 1781–1800. https://doi.org/10.1016/j.rse.2011.02.019

Müller, C., Elliott, J., Chryssanthacopoulos, J., Arneth, A., Balkovic, J., Ciais, P., … Yang, H. (2017). Global gridded crop model evaluation: Benchmarking, skills, deficiencies and implications. *Geoscientific Model Development*, *10*, 1403–1422. https://doi.org/10.5194/gmd-10-1403-2017

Olesen, J. E., Trnka, M., Kersebaum, K. C., Skjelvåg, A. O., Seguin, B., Peltonen-Sainio, P., … Micale, F. (2011). Impacts and adaptation of European crop production systems to climate change. *European Journal of Agronomy*, *34*, 96–112. https://doi.org/10.1016/j.eja.2010.11.003

Ordóñez, R. A., Savin, R., Cossani, C. M., & Slafer, G. A. (2015). Yield response to heat stress as affected by nitrogen availability in maize. *Field Crops Research*, *183*, 184–203. https://doi.org/10.1016/j.fcr.2015.07.010

Parent, B., & Tardieu, F. (2012). Temperature responses of developmental processes have not been affected by breeding in different ecological areas for 17 crop species. *New Phytologist*, *194*, 760–774.

Ponce-Campos, G. E., Moran, M. S., Huete, A., Zhang, Y., Bresloff, C., Huxman, T. E., … Starks, P. J. (2013). Ecosystem resilience despite large-scale altered hydroclimatic conditions. *Nature*, *494*, 349–352. https://doi.org/10.1038/nature11836

Rahmstorf, S., & Coumou, D. (2011). Increase of extreme events in a warming world. *Proceedings of the National Academy of Sciences*, *108*, 17905–17909. https://doi.org/10.1073/pnas.1101766108

Rezaei, E. E., Siebert, S., Hüging, H., & Ewert, F. (2018). Climate change effect on wheat phenology depends on cultivar change. *Scientific Reports*, *8*(1), 4891. https://doi.org/10.1038/s41598-018-23101-2

Rezaei, E. E., Webber, H., Gaiser, T., Naab, J., & Ewert, F. (2015). Heat stress in cereals: Mechanisms and modelling. *European Journal of Agronomy*, *64*, 98–113. https://doi.org/10.1016/j.eja.2014.10.003

Rosenzweig, C., Jones, J. W., Hatfield, J. L., Ruane, A. C., Boote, K. J., Thorburn, P., … Winter, J. M. (2013). The Agricultural Model Intercomparison and Improvement Project (AgMIP): Protocols and pilot studies. Special Issue: Agricultural prediction using climate model ensembles. *Agricultural and Forest Meteorology*, *170*, 166–182. https://doi.org/10.1016/j.agrformet.2012.09.011

Rötter, R. P., Carter, T. R., Olesen, J. E., & Porter, J. R. (2011). Crop-climate models need an overhaul. *Nature Climate Change*, *1*, 175–177. https://doi.org/10.1038/nclimate1152

Ruiz-Vera, U. M., Siebers, M. H., Jaiswal, D., Ort, D. R., & Bernacchi, C. J. (2018). Canopy warming accelerates development in soybean and maize, offsetting the delay in soybean reproductive development by elevated CO_2 concentrations. *Plant, Cell & Environment*, *1*(12):2806–2820. https://doi.org/10.1111/pce.13410

Sacks, W. J., Deryng, D., Foley, J. A., & Ramankutty, N. (2010). Crop planting dates: An analysis of global patterns. *Global Ecology Biogeography*, *19*, 607–620. https://doi.org/10.1111/j.1466-8238.2010.00551.x

Sánchez, B., Rasmussen, A., & Porter, J. R. (2014). Temperatures and the growth and development of maize and rice: A review. *Global Change Biology*, *20*, 408–417. https://doi.org/10.1111/gcb.12389

Schauberger, B., Archontoulis, S., Arneth, A., Balkovic, J., Ciais, P., Deryng, D., … Frieler, K. (2017). Consistent negative response of US crops to high temperatures in observations and crop models. *Nature. Communications*, *8*, 13931. https://doi.org/10.1038/ncomms13931

Schlenker, W., & Roberts, M. J. (2009). Nonlinear temperature effects indicate severe damages to U.S. crop yields under climate change. *Proceedings of the National Academy of Sciences*, *106*, 15594–15598. https://doi.org/10.1073/pnas.0906865106

Siebers, M. H., Slattery, R. A., Yendrek, C. R., Locke, A. M., Drag, D., Ainsworth, E. A., … Ort, D. R. (2017). Simulated heat waves during maize reproductive stages alter reproductive growth but have no lasting effect when applied during vegetative stages. *Agriculture, Ecosystems and Environment*, *240*, 162–170. https://doi.org/10.1016/j.agee.2016.11.008

Siebers, M. H., Yendrek, C. R., Drag, D., et al. (2015). Heat waves imposed during early pod development in soybean (*Glycine max*) cause significant yield loss despite a rapid recovery from oxidative stress. *Global Change Biology*, *21*(8), 3114–3125.

Tack, J., Barkley, A., & Nalley, L. L. (2015). Effect of warming temperatures on US wheat yields. *Proceedings of the National Academy of Sciences*, *112*, 6931–6936. https://doi.org/10.1073/pnas.1415181112

Tao, F., Yokozawa, M., Xu, Y., Hayashi, Y., & Zhang, Z. (2006). Climate changes and trends in phenology and yields of field crops in China, 1981–2000. *Agricultural and Forest Meteorology*, *138*, 82–92. https://doi.org/10.1016/j.agrformet.2006.03.014

Tollenaar, M., & Wu, J. (1999). Yield improvement in temperate maize is attributable to greater stress tolerance. *Crop Science*, *39*, 1597–1604. https://doi.org/10.2135/cropsci1999.3961597x

USDA. (2015). *World Agricultural Supply and Demand Estimates*. Washington, D.C.: United States Department of Agriculture, 1–40.

Wahid, A., Gelani, S., Ashraf, M., & Foolad, M. R. (2007). Heat tolerance in plants: An overview. *Environmental and Experimental Botany*, *61*, 199–223. https://doi.org/10.1016/j.envexpbot.2007.05.011

Warszawski, L., Frieler, K., Huber, V., Piontek, F., Serdeczny, O., & Schewe, J. (2014). The Inter-Sectoral Impact Model Intercomparison Project (ISI–MIP): Project framework. *Proceedings of the National Academy of Sciences*, *111*, 3228–3232. https://doi.org/10.1073/pnas.1312330110

Webber, H., Martre, P., Asseng, S., Kimball, B., White, J., Ottman, M., … Ewert, F. (2017). Canopy temperature for simulation of heat stress in irrigated wheat in a semi-arid environment: A multi-model comparison. *Field Crops Research*. *202*, 21–35. https://doi.org/10.1016/j.fcr.2015.10.009

Zhu, P., Jin, Z., Zhuang, Q., Ciais, P., Bernacchi, C., Wang, X., … Lobell, D. (2018). The important but weakening maize yield benefit of grain filling prolongation in the US Midwest. *Global Change Biology*, *24*(10):4718–4730.https://doi.org/10.1111/gcb.14356

SUPPORTING INFORMATION

Additional supporting information may be found online in the Supporting Information section at the end of the article.

How to cite this article: Zhu P, Zhuang Q, Archontoulis SV, Bernacchi C, Müller C. Dissecting the nonlinear response of maize yield to high temperature stress with model-data integration. *Glob Change Biol*. 2019;00:1–15. https://doi.org/10.1111/gcb.14632